Macrophage α-Actinin Is Not a Calcium-Modulated Actin-Binding Protein†

M. Pacaud* and M. C. Harricane

Centre de Recherches de Biochimie Macromolèculaire, CNRS UPR 9008, INSERM U 249, Université de Montpellier I, BP 5051, 34033 Montpellier Cedex, France

Received June 18, 1992; Revised Manuscript Received October 9, 1992

ABSTRACT: α-Actinin was purified from rabbit macrophages to apparent homogeneity by a procedure designed to remove other actin-binding proteins. Large bundles of filaments were formed when 1 molecule of α-actinin interacted with 10–12 actin monomers. This process involved the successive occupancy of two classes of actin-binding sites with different affinities. The apparent K_d of α-actinin for F-actin was unaffected by the addition of 25 μM free Ca^{2+}. Analysis of the influence of increasing Ca^{2+} concentrations on α-actinin–F-actin interactions by low-speed sedimentation assays, low-shear viscosity, and electron microscopy indicated that Ca^{2+} had a small inhibitory effect in the approximate range of 50–1000 μM. Furthermore, the ability of α-actinin to assemble actin filaments into bundles was apparently inhibited only at Ca^{2+} concentrations which also affected the physical properties of F-actin alone. α-Actinin immobilized on a nitrocellulose membrane did not bind detectable amounts of Ca^{2+}. Nevertheless, Ca^{2+} or Mg^{2+} binding to α-actinin induced small decreases in the fluorescence emission intensity of tryptophan and tyrosine residues. The maximal change induced by Mg^{2+} was smaller than that observed with Ca^{2+}, but Ca^{2+} and Mg^{2+} effects were abolished by the addition of 140 mM KCl. Under near-physicological ionic conditions, Ca^{2+}-binding sites with an apparent K_d higher than 80–100 μM could not be detected. The results on the functional and physical properties of α-actinin are consistent with the hypothesis that Ca^{2+} decreases α-actinin–F-actin interactions by acting both on actin filaments and on cross-linking molecules. Although this conclusion is in contradiction with the generally accepted idea that αA is a Ca^{2+}-regulated actin-binding protein, it could be predicted from the primary sequence of the two EF-hand-like motifs in the α-actinin monomer [Arimura et al. (1988) *Eur. J. Biochem. 177,* 649–655] based on the crucial role of some Ca^{2+}-binding residues as recently demonstrated by point mutations in Ca^{2+}-binding sites of calmodulin [Haiech et al. (1991) *J. Biol. Chem. 266,* 3427–3431]. It is also in agreement with our previous finding that Ca^{2+} does not affect the behavior of α-actinin in actin gel networks from macrophage cytosolic extracts [Pacaud & Harricane (1987) *J. Cell Sci. 88,* 81–94].

There is much indirect evidence suggesting that Ca^{2+} is involved in the initiation of cytoskeletal reorganization in macrophages and neutrophils in response to chemotractant or phagocytic *stimuli* (Sklar et al., 1985; Howard & Oresajo, 1985; Omann et al., 1987). The dynamic properties of microfilaments are thought to be mediated by controlled variations in the interactions of actin with actin-associated proteins. Several types of actin-related proteins have been characterized from macrophages and other cells (Weeds, 1982; Stossel et al., 1985; Pollard & Copper, 1986). It has been proposed that one of these [α-actinin (αA)][1] might contribute to the Ca^{2+}-sensitive gelation of actin in cytoplasmic extracts and possibly to the regulation of microfilament architecture in nonmuscle cells (Burridge & Feramisco, 1981a; Craig & Pollard, 1982). In contrast to skeletal and smooth muscle proteins (Ebashi et al., 1964; Endo & Masaki, 1982), nonmuscle αA's isolated from HeLa cells (Burridge & Feramisco, 1981b), brain (Duhaiman & Bamburg, 1984), macrophages (Bennet et al., 1984), platelets (Rosenberg et al., 1981; Landon et al., 1985), and liver (Ohtaki et al., 1985) have all been found to cross-link actin filaments in a Ca^{2+}-dependent manner. It is generally assumed that Ca^{2+} prevents the binding of nonmuscle αA to actin, although convincing evidence for such a mechanism has not yet been reported.

αA is a dumbbell-shaped molecule composed of two identical subunits, of ~100 kDa each, oriented in an antiparallel fashion (Wallraff et al., 1986; Witke et al., 1986). On the basis of the complete αA amino acid sequence from different sources (Baron et al., 1987); Noegel et al., 1987; Arimura et al., 1988), it is now clear that the αA monomer is composed of 3 domains: an NH_2-terminal actin-binding domain, an extended rodlike domain with 4 internal 122 amino acid repeats, and a COOH-terminal region containing a pair of presumptive helix–loop–helix Ca^{2+}-binding motifs, often referred to as EF-hands [for a recent review, see Strynadka and James (1989)]. Six residues in the Ca^{2+}-binding loop are involved in calcium ligation through the use of oxygen-containing amino acid side chains or α-carbonyl oxygens from the polypeptide backbone. The six calcium ligation residues are at positions 1, 3, 5, 7, 9, and 12 in the amino sequence of the loop. The residues at positions 1 and 12 are invariably Asp and Glu. The primary sequence of the two loop regions on the αA monomer displays some important differences with that of typical EF-hand calcium-binding proteins. Chicken smooth muscle and fibroblast αA's are 98% identical, differing only in the loop region of the first presumptive Ca^{2+}-binding motif (Arimura et al., 1988; Blanchard et al., 1989). However, in each αA isoform, this loop is missing a Ca^{2+} ligation residue. The fibroblast αA loop has a Gly residue at position 9, whereas the smooth muscle αA loop has a Met residue at position 7

† This work was supported by the CNRS.

* To whom correspondence should be addressed.

[1] Abbreviations: αA, α-actinin; 70 kDa, 70 000 dalton; EGTA, ethylene glycol bis(β-aminoethyl ether)-*N,N,N′,N′*-tetraacetic acid; EDTA, ethylenediaminetetraacetic acid; HEPES, *N*-(2-hydroxyethyl)piperazine-*N′*-2-ethanesulfonic acid; DFP, diisopropyl fluorophosphate; TLCK, tosyl-L-lysine chloromethyl ketone; MOPS, 3-(*N*-morpholino)propanesulfonic acid; SDS, sodium dodecyl sulfate; PAGE, polyacrylamide gel electrophoresis.

0006-2960/93/0432-363$04.00/0

and an Asp instead of a Glu residue at position 12. The loop of the second EF-hand-like motif possesses three amino acid substitutions which distinguish it from strong Ca^{2+}-binding sites. It has Met and Val residues at positions 5 and 7, respectively, and, more significantly, an Ala residue at position 12 instead of the invariant Glu. Haiech et al. (1991) recently reported that the Glu → Ala mutation at position 12 of the Ca^{2+}-binding loop in the second or fourth sites of calmodulin resulted in the loss of calcium-selective binding at each pair of sites (sites I and II or sites III and IV). This is an essential finding because it demonstrates for the first time coupling between pairs of sites in each half of calmodulin and residue 12 of the calcium ligation structure. Accordingly, on the basis of this new information, it could be predicted that the EF-hand-like motifs of fibroblast and smooth αA probably have a low Ca^{2+}-binding affinity. However, this would be in contradiction with the high Ca^{2+} sensitivity reported for αA isoforms from vertebrate nonmuscle cells.

In previous studies on the Ca^{2+}-dependent regulation of the gelation reaction in macrophage cytosolic extracts, we observed that the binding of αA to actin gel networks was insensitive to calcium. In addition, we demonstrated that a 70-kDa actin-bundling protein was the only component which lost its affinity for actin filaments at physiological concentrations of calcium (Pacaud & Molla, 1987; Pacaud & Harricane, 1987). These observations and published information of EF-hand calcium-binding motifs prompted us to reinvestigate the mechanism by which calcium effects the in vitro formation of αA–F-actin complexes. In this report, we describe the purification and characterization of αA from rabbit alveolar macrophages. We also assess the effects of Ca^{2+} on the functional and spectral properties of αA, in an attempt to determine whether the Ca^{2+}-induced changes in αA–F-actin interactions are a consequence of ions binding to αA molecules. The results are discussed in comparison with those reported by other investigators.

MATERIALS AND METHODS

All chemicals were reagent grade or the purest commercially available. $^{45}CaCl_2$ (34.1 mCi/mg) was purchased from New England Nuclear. Calmodulin from bovine testis was a kind gift from Jean-Paul Capony as prepared by the method of Autric et al. (1980). All buffers were made with ultrapure water (Milli-Q instrument from Millipore Corp.). Actin was prepared from rabbit skeletal muscle using a modification of the procedure of Spudich and Watt (1971) with one cycle of polymerization and depolymerization from 0.8 M KCl. Monomeric actin was further purified by gel filtration on a Sephacryl S-200 column in a buffer containing 2 mM Tris-HCl, 0.1 mM $CaCl_2$, 0.2 mM ATP, 0.02 mM dithiothreitol, and 0.02% NaN_3, pH 7.8.

Purification of α-Actinin. All purification procedures were performed at 4 °C. Alveolar macrophages were obtained from New Zealand white rabbits, treated with 0.25 mM DFP for 10 min, and washed twice with an equal volume of ice-cold 0.15 M NaCl solution. The packed cells were broken in a Potter homogenizer with 1.5 volumes of buffer A (15 mM HEPES, 0.34 M sucrose, 6 mM EGTA, 1 mM EDTA, 2 mM NaN_3, and 1 mM dithiothreitol, pH 7.2) supplemented with 1 mM DFP, 0.02 mM TLCK, and pepstatin A (2 μg mL^{-1}). The cell lysate was centrifuged at 12000*g* for 15 min at 4 °C, and the supernatant was collected. The pellet was resuspended, as described above, in a volume of extraction buffer equal to the volume of the initial cell pellet and centrifuged again. The two supernatants were combined and clarified by centrifugation at 120000*g* for 1 h at 4 °C. Solid KCl was added to the clear cytosolic extract at a final concentration of 0.6 M and stirred for 2 h.

Ammonium Sulfate Fractionation. The 0.6 M KCl extract was mixed with solid ammonium sulfate to 25% saturation and stirred. The pH was brought to 7.2 with 0.5 M NaOH; the suspension was stirred for 45 min and centrifuged at 27000*g* for 10 min. Ammonium sulfate was added to the supernatant to 38% saturation; the suspension was stirred for 1 h and recentrifuged. The pellet was dissolved in buffer B (0.2 volume of the cytosolic extract) containing 10 mM HEPES, 0.25 M sucrose, 50 mM KCl, 0.2 mM dithiothreitol, and 2 mM NaN_3, pH 7.2, supplemented with protease inhibitors as indicated above. The suspension was dialyzed against 200 volumes of buffer B for 2 h. The precipitate, consisting essentially of F-actin and myosin, was removed by centrifugation. This supernatant was diluted 3-fold with buffer B brought to 0.6 M in KCl, and again ammonium sulfate was added to 38% saturation. The precipitate was dissolved in a minimum volume of buffer C (20 mM Tris-HCl/2 mM NaN_3, pH 7.6) supplemented with protease inhibitors. The protein solution was dialyzed against 200 volumes of buffer C for 4 h with one change of buffer. The final precipitate that formed during dialysis was removed by centrifugation at 120000*g* for 2 h.

DEAE-Trisacryl Chromatography. The clear supernatant (125 mg of protein) was diluted 2-fold with buffer C (supplemented with protease inhibitors) and applied to a DEAE-Trisacryl (LKB) column equilibrated with buffer C. The column was washed with this buffer until the absorbance at 280 nm became constant and then eluted with a linear gradient of KCl from 60 to 320 mM in buffer D (20 mM Tris-HCl, 2 mM EGTA, and 0.2 mM dithiothreitol, pH 7.6). αA emerged at a KCl concentration of about 210 mM. The pooled fractions were supplemented with protease inhibitors (0.1 mM DFP, 0.05 mM TLCK, and 0.5 mg mL^{-1} soybean trypsin inhibitor) and dialyzed for 3 h against 50 volumes of buffer D containing 30 mM KCl and 1 mM EGTA. The dialyzed solution was then concentrated by chromatography through a small column of DEAE-Trisacryl (1.5 mL) equilibrated with the dialysis buffer. After the column was washed with 3 volumes of this buffer, adherent proteins were eluted to a sharp peak by increasing the KCl concentration stepwise to 320 mM.

Size-Exclusion Chromatography. The concentrated protein solution was dialyzed against buffer E (15 mM HEPES, 0.8 M KCl, 0.1 mM dithiothreitol, and 2 mM NaN_3, pH 7.2) for 3 h. The dialyzed solution was supplemented with the three protease inhibitors indicated above and centrifuged at 120000*g* for 2 h. The clear supernatant was applied to a column of Ultrogel AcA-34 (1.6 × 95 cm) previously equilibrated with buffer E. Using the same buffer as eluant, 1.5-mL fractions were collected at a flow rate of 16 mL/h. The fractions containing αA were pooled and concentrated over DEAE-Trisacryl as described above. The eluate was then dialyzed overnight against 10 mM HEPES, 10% glycerol (v/v), 50 mM KCl, and 0.1 mM dithiothreitol, pH 7, divided into aliquots, and stored at −80 °C.

F-Actin bundling was estimated by a low-speed sedimentation assay. Monomeric actin (final concentration 400 μg mL^{-1}) was polymerized at room temperature in the presence of increasing concentrations of purified αA in 100 μL of buffer F (15 mM HEPES, 2 mM $MgCl_2$, 50 mM KCl, 0.1 mM dithiothreitol, and 0.2 mM ATP, pH 7.2). After incubation for 3 h at 25 °C, the reaction mixtures were centrifuged at 16000*g* for 12 min at 4 °C. The supernatants were carefully

withdrawn and the pellets suspended in 20 mM HEPES, pH 7. Both supernatants and pellets were dissolved in the same volume of SDS sample buffer (1% SDS, 10% glycerol, 50 mM dithiothreitol, 40 mM Tris-HCl, and 0.001% bromophenol blue, pH 6.8). Samples were run on 10% SDS–polyacrylamide gels, stained with Coomassie Blue, and quantified by scanning densitometry using purified actin and αA as standards.

F-Actin binding to αA was measured by high-speed centrifugation. F-Actin at 400 μg mL^{-1} was incubated with 0–150 μg mL^{-1} αA. After 3 h at 25 °C, the mixtures were centrifuged at 120000*g* for 1 h at 4 °C. Supernatants were separated from pellets, and both fractions were suspended in an equivalent volume of sample buffer for SDS–PAGE analysis. Actin and αA concentrations were determined by scanning densitometry.

To determine the pH dependence of the binding of αA to F-actin, 20 mM MOPS and 10 mM HEPES plus 10 mM Tris-HCl were substituted for the 15 mM HEPES in buffer F, and the pH was adjusted to between 6.2 and 7.6. Assays were carried out at a constant αA:actin molar ratio of 1:10 in the presence of 1 mM EGTA.

Apparent viscosity was measured at low shear rates by the falling ball technique as described by MacLean-Flechter and Pollard (1980). Increasing concentrations of αA were mixed with a constant amount of G-actin (final concentration 0.4 mg mL^{-1}) in buffer F containing various Ca^{2+}:EGTA ratios maintaining [EGTA] at 1 mM. Samples were then drawn into 100-μL glass capillaries and kept at 25 °C for 3 h before measurements. A calibration curve was established using a series of glycerol solutions (10–60%) of known viscosities. This approach yielded a semiquantitative comparison of the consistence of non-Newtonian solutions.

Removal of Contaminating Metal. The buffer solution used for calcium-binding studies was 20 mM HEPES/NaOH buffer, pH 7.0, containing 10% glycerol. All buffer and reagent solutions were passed through a Chelex-100 column (Bio-Rad) and stored in plasticware. Cuvettes for spectrophotometric measurements and plasticware were soaked for 2–4 h with 50% nitric acid and extensively washed with ultrapure water. Dialysis tubing was boiled in 5% $NaHCO_3$ and 0.1 mM EDTA and extensively rinsed. αA was freed from Ca^{2+} by dialysis, at 0–4 °C for 18 h, against 100 volumes of the buffer used for fluorescence measurements containing 1% Chelex equilibrated with the same buffer. The buffer and Chelex were changed once after 12-h dialysis.

Fluorescence Measurements. Fluorescence spectra were obtained with a Perkin Elmer LS50 spectrofluorometer. Spectra were recorded after successive additions of 4–20-μL aliquots of 0.1, 1, and 10 mM $CaCl_2$ solutions and corrected for dilutions. Excitation was performed at 270 or 290 nm for tyrosine and tryptophan, respectively, and fluorescence was observed at 310 or 330 nm.

Free Ca^{2+} ion concentrations were determined using the computer program of Haiech et al. (1979). The apparent dissociation constant used for EGTA-Ca^{2+} was 3×10^{-7} M at pH 7.2 and in the presence of 2 mM $MgCl_2$.

Protein Determination. The concentration of monomeric actin was determined from its optical density using an extinction coefficient of 0.65 at 290 nm for 1 mg mL^{-1} solution of actin. All other protein concentrations were measured as per Lowry et al. (1951) with bovine serum albumin as standard.

Polyacrylamide gel electrophoresis was carried out according to Leammli (1970) with 10% polyacrylamide gels. For quantitative densitometry, stained gels were scanned with a Shimadzu densitometer (Model CS-930) equipped with a computer program.

Electron microscopy was carried out as described earlier (Pacaud & Harricane, 1987) using a JEOL 2000 EX instrument.

RESULTS

Purification of Macrophage α-Actinin. The new procedure for the purification of αA from macrophage cytosolic extracts outlined under Materials and Methods was devised (a) to increase the yield of this protein and (b) to ensure maximum separation from all other actin-binding proteins. The 25–38% ammonium sulfate fraction was applied to a DEAE-Trisacryl column, and the adsorbed proteins were eluted with a KCl gradient. In addition to a large amount of actin, the ammonium sulfate pellet contained several actin-associated proteins including myosin and filamin [previously designated as "macrophage actin-binding protein" by Hartwig and Stossel (1981)]. These two contaminants eluted with the first peak, while αA emerged at the end of the second peak at about 210 mM KCl (Figure 1A,C). The final purification of αA was achieved by molecular sieve chromatography on Ultrogel AcA-34 (Figure 1B,D). As shown in Figure 1E, fractions concentrated from the Ultrogel column appeared to be better than 95% electrophoretically pure, as determined by quantitative densitometry (not shown). The purified protein was frozen in liquid nitrogen and stored at −80 °C. It was generally kept for 3–6 weeks without any evidence of proteolysis and loss of functional activity.

The purification results are summarized in Table I. In a typical preparation, 0.8–1 mg of αA can be obtained from 520 mg of cytosolic proteins. On the basis of densitometry scans of Coomassie Blue-stained SDS–polyacrylamide gels, this protein represented 0.7–0.8% of all protein in the cytosolic extracts.

Properties of Purified α-Actinin. As expected, the purified protein migrated as a (100 000 ± 6000)-dalton (100-kDa) polypeptide on both 6 and 9% SDS–polyacrylamide gels. The 100-kDa polypeptide had an isoelectric point of 6.4 which focused as a single component on two-dimensional polyacrylamide gels (data not shown).

αA was tested for its ability to bundle actin filaments by low-speed sedimentation as indicated under Materials and Methods. The assay was set up to allow for the separation of αA–F-actin complexes from unbound protein. Under the centrifugation conditions used, no significant amounts of either αA or F-actin were pelleted. However, F-actin together with increasing amounts of αA was sedimented by increasing the molar ratio of αA to actin in a range that varied from 1:20 to 1:12 (data not shown). At molar ratios greater than about 1:12, the αA-induced increase in F-actin sedimentability remained relatively constant, suggesting that the αA-binding sites on actin had become saturated.

The influence of pH and temperature was also assessed in order to obtain optimal conditions for measuring αA–F-actin interactions. On the basis of viscosimetric studies at low shear forces, Bennet et al. (1984) reported that the ability of αA to cross-bridge actin filaments was higher at 4 °C than at 21 °C and was abolished at 37 °C. We therefore estimated the extent of bundle formation at a constant αA to F-actin molar ratio of 1:10, after 3-h incubation at different temperatures. Actin bundling increased 3–4-fold when temperatures were increased up to 21 °C; it then remained quite unchanged up to 37 °C (Table II). However, the rate of actin assembly occurred faster at 37 °C than at 21 °C because maximal

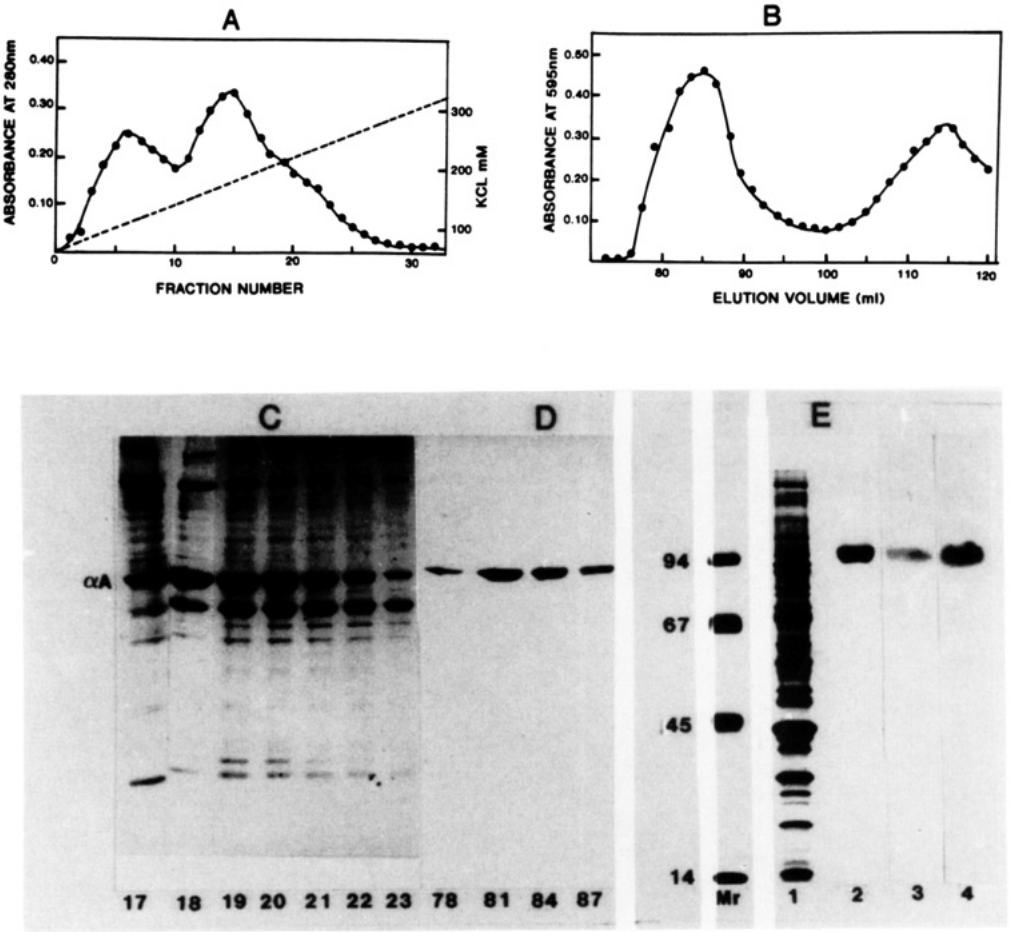

FIGURE 1: Purification of macrophage αA by chromatography on DEAE-Trisacryl and Ultrogel AcA-34. (A) Elution profile of the DEAE-Trisacryl column. Proteins resulting from the last ammonium sulfate fractionation (see Materials and Methods) were applied to a DEAE-Trisacryl column (3.6 × 2.5 cm) previously equilibrated with buffer C. After the absorbance of the eluant at 280 nm had returned to base line, the column was eluted with a 180-mL linear KCl gradient from 60 to 320 mM. Fractions of 3.5 mL each were analyzed by electrophoresis on 10% polyacrylamide gels and tested for their ability to bind F-actin by sedimentation at high speed. (C) SDS–PAGE of the fractions containing αA eluted from DEAE-Trisacryl. The numbering of the lanes corresponds with the fraction numbers. (B) Elution profile of the Ultrogel AcA-34 column. Fractions 18–23 from the DEAE-Trisacryl column were pooled and concentrated to a protein concentration of 0.8 mg mL^{-1}. The protein solution was then chromatographed on a 1.6 × 95 cm column of Ultrogel AcA-34. (E) Protein composition and immunoblot analysis of fractions before and after purification. Protein fractions were subjected to SDS–PAGE on 5–18% gradient gels and either stained with Coomassie Blue (lanes 1 and 2) or transferred on nitrocellulose paper (lanes 3 and 4). The filters were then incubated with polyclonal anti-α-actinin antibodies. Bound antibodies were detected with peroxidase-labeled goat anti-rabbit IgG as previously described (Pacaud, 1986). Samples: lanes 1 and 3, protein recovered after ammonium sulfate precipitation; lanes 2 and 4, fractions collected from Ultrogel AcA-34 and eluted between 81 and 87 mL (22 μg of protein was used in lane 2 and 10 μg in lane 4). Molecular weight markers (M_r) (×10^{-3}) are as follows: phosphorylase *b*, 94 000; bovine serum albumin, 67 000; ovalbumin, 45 000; α-lactalbumin, 14 000.

Table I: Purification of Macrophage α-Actinin

fraction	total protein (mg)	αA[a] (mg)	yield (%)
cytosolic extract	521	3.9	100
25–38% ammonium sulfate	124.5	3.2	82
DEAE-Trisacryl	3.6	1.2	31
Ultrogel AcA-34	0.9	0.9	23

[a] The αA content of each fraction was determined by quantitative densitometry of Coomassie Blue-stained gels as described under Materials and Methods. αA in cytosolic extracts and ammonium sulfate fractions was identified by immunoblotting using monospecific αA antibodies (Pacaud, 1986). The data represent the average of three separate preparations from 15–20 mL of packed cells.

Table II: Influence of Temperature and pH on α-Actinin–F-Actin Interactions[a]

temp (°C)	% of pelleted actin	pH	% of pelleted αA	temp (°C)	% of pelleted actin	pH	% of pelleted αA
7	30	6.3	32	30	92	6.8	98
15	62	6.5	60	37	96	7	94
21	92	6.7	78			7.5	98

[a] The bundling activity of αA at different temperatures was measured by low-speed sedimentation. Polymerized actin at 3.5 mM and αA at 3 mM were incubated for 2 h at each temperature in buffer F (15 mM HEPES, 2 mM $MgCl_2$, 50 mM KCl, 0.1 mM dithiothreitol, and 0.2 mM ATP) with 0.1 mM EGTA. Calculations were based throughout on a molecular mass of 43 000 for monomeric actin and 200 000 for αA. The reaction mixtures were centrifuged at 16000*g* for 12 min, and the supernatants and pellets were analyzed by SDS–PAGE. The influence of pH on the ability of αA to bind to F-actin was assessed at 25 °C in similar conditions except that F-actin was pelleted at 120000*g* for 30 min. F-Actin bound to αA was calculated by subtracting the free actin in supernatants from the total actin used in the binding assay.

bundle formation was reached at 10–15 min instead of ~1 h. These results, unlike those of Bennet et al. (1984), thus indicate that the assembly of actin filaments by αA occurs at physiological temperatures. The pH dependence of αA binding to F-actin was assessed at 25 °C by high-speed sedimentation. The amount of αA which cosedimented with F-actin increased sharply from pH 6.3 to 6.8 and then remained quite constant at pH 7.5 (Table II). Taken as a whole, these results indicate that purified macrophage αA behaves like αA

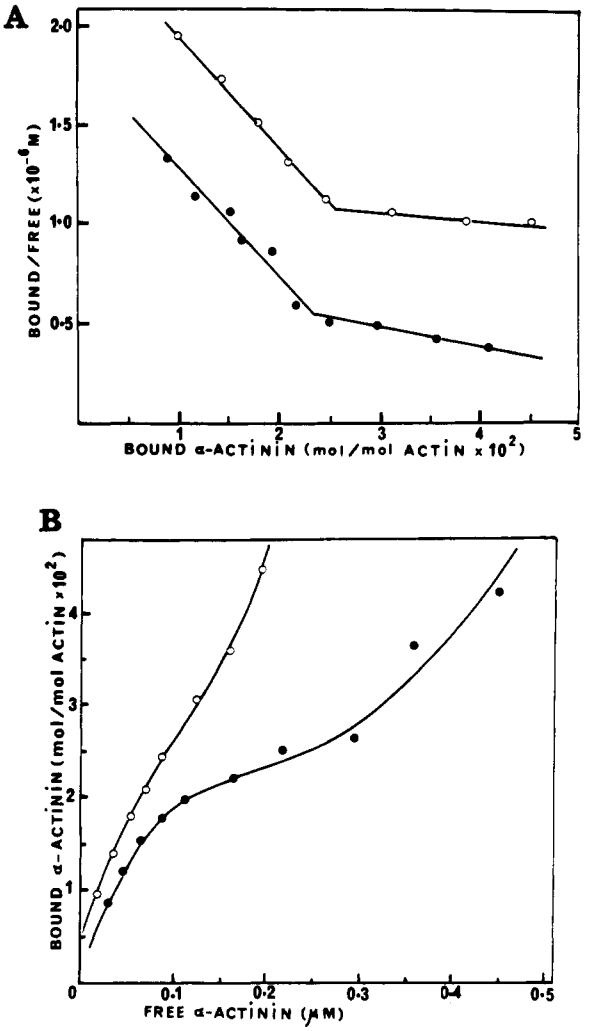

FIGURE 2: Binding of αA to F-actin at pH 7.0 and 25 °C. Various amounts of αA were mixed with F-actin (9.3 μM) in buffer F containing 0.1 mM EGTA without Ca^{2+} (●) and with 25 μM free Ca^{2+} (○). Bound αA was measured by a high-speed sedimentation assay as indicated under Materials and Methods. Each point represents the average value obtained from two duplicate trials within a single experiment. Data were plotted according to Scatchard's representation in (A) or directly in (B). The effect of Ca^{2+}, at concentrations higher than 25 μM, on the stoichiometry of binding could not be assessed using this assay because Ca^{2+} decreased the stability of α-actinin–F-actin structures at high shear forces.

from platelets and chicken gizzard (Landon et al., 1985; Meyer & Aebi, 1990).

Influence of Calcium on α-Actinin–F-Actin Interactions. The binding of αA to F-actin was determined, both in the absence and in the presence of 25 μM free Ca^{2+}, by high-speed rather than low-speed sedimentation in order to pellet all sizes and types of αA–F-actin complexes. The results of each experiment were expressed as the molar ratio of pelleted αA (bound) to total actin and plotted versus the amount of αA remaining in the supernatant (free). Further analysis of the binding of αA to F-actin by the Scatchard method revealed two major classes of binding sites with apparent K_d values of about 5.5 and 10 μM, respectively, as illustrated in Figure 2. The dissociation constants measured with or without Ca^{2+} were not significantly different. However, Ca^{2+} caused about 30% increase in the binding stoichiometry. In fact, this might reflect some differences in the stability of αA–F-actin structures which were formed in the presence and absence of Ca^{2+}. Extrapolation of the binding data, obtained in the presence of EGTA alone, indicated that high-affinity sites were saturated when 1 αA molecule was bound for each 25–30 actin monomers while low-affinity sites were almost saturated when 1 αA molecule was bound for each 12–15 actin monomers.

Table III: Estimation of the Effect of Ca^{2+} on the αA-Induced Increase in Low-Speed Sedimentability of F-Actin[a]

free Ca^{2+} concn (μM)	actin pelleted in control samples (%)	actin pelleted with αA (%)	αA-induced increase in pelleted actin (%)	extent of actin assembly (%)
0	11.7	66.7	55.0	100
0.5	11.2	65.4	54.2	98.5
2.9	12.6	67.3	54.7	99.4
25	16.7	70.6	53.9	98.0
50	20.1	71.4	51.3	92.4
100	21.2	70.5	49.3	89.6
500	22.3	68.6	46.3	84.0
1000	23.8	66.2	42.4	77.2

[a] Rabbit muscle actin was polymerized after addition of 0.1 M EGTA (for Ca^{2+} chelation) and dialyzed for 5 h against buffer F. The resulting solution was brought to a final F-actin concentration of 9.3 μM, divided in two sets of samples, and added with sufficient amounts of $CaCl_2$ and EGTA to obtain the free Ca^{2+} concentrations indicated. One set of samples was incubated alone, while the other was incubated in the presence of α-actinin at a final concentration of 1.1 μM. After low-speed centrifugation, the supernatants and pellets were analyzed by SDS–PAGE and densitometric scanning. Similar results were obtained from two different preparations of actin and α-actinin. The amount of α-actinin pelleted with F-actin remained relatively constant in each experiment. This indicates that Ca^{2+} affects the α-actinin–F actin interactions outside a physiological range of concentrations.

Because αA is a constituent of actin stress fibers in cultured cells (Lazarides & Burridge, 1975; Pavalko & Burridge, 1991), it seems more physiologically relevant to investigate how αA–F-actin interactions are affected by Ca^{2+} under optimal conditions of bundle formation. Low-speed sedimentation was used to measure bundling activity in order to minimize the influence of shearing forces on the structural integrity of bundles formed in the presence and absence of Ca^{2+}. The results of each experiment were expressed as the ratio of pelleted actin to total actin after incubation in the absence or presence of saturating amounts of αA. As Ca^{2+} was found to increase the sedimentability of F-actin in the absence of αA, the extent of bundle formation was calculated arbitrarily from the difference in the amount of F-actin pelleted with and without αA. As shown in Table III, Ca^{2+} did not affect the bundling activity of αA up to a free concentration of 50 μM. However, at higher concentrations, it had a small and progressive inhibitory effect. Thus, a 10% reduction was observed in the presence of 0.1 mM free Ca^{2+} and a decrease of only 23% at 1 mM.

The [Ca^{2+}] dependence of the αA:F-actin ratio was examined by low-shear viscosity because this procedure provides an approximate measurement of the initial cross-bridging of actin filaments and the bundling process. In the absence of Ca^{2+}, αA caused biphasic enhancement in the apparent viscosity of F-actin. A linear relationship was observed at αA to actin molar ratios lower than 1:30–1:35, i.e., below the critical ratio for bundle formation. Identical variations were observed in the presence of 25 μM free Ca^{2+} (Figure 3). However, at 100 μM free Ca^{2+} and higher, the viscosity of αA–F-actin mixtures exhibited a complex dependence on the αA:actin ratio. Increasing the molar ratios of αA to actin from 1:35 to 1:12 resulted in a gradual and complete decrease in the apparent viscosity of F-actin bundles as compared to the value obtained for F-actin alone. At

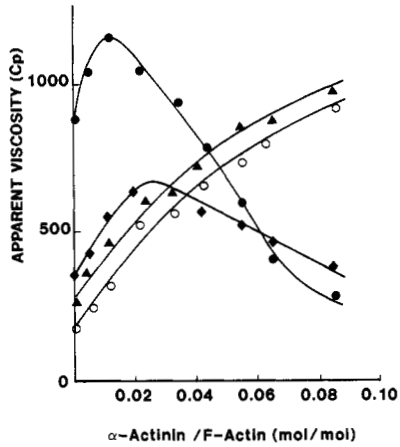

FIGURE 3: Effects of αA concentrations on the apparent viscosity of F-actin with or without Ca^{2+}. Gel-filtered G-actin from rabbit skeletal muscle (final concentration 0.4 mg/mL) was mixed with various amounts of αA, and polymerization was induced by addition of salts. The apparent viscosity was measured after 3-h incubation at 25 °C and pH 7, as indicated under Materials and Methods. The samples contained either 1 mM EGTA (○) or 25 (▲), 100 (♦) or 1000 μM (●) free Ca^{2+}.

millimolar Ca^{2+}, the apparent viscosity of the mixtures dropped to an even lower level than that of the F-actin control. This drop in the apparent viscosity was not due to shortening or depolymerization of actin filaments, since both electron microscopy and sedimentation analysis showed the presence of assembled filaments and fast sedimentable proteins. Since Ca^{2+} increased the apparent viscosity of F-actin in the absence of αA, subsequent decrease in actin viscosity might have been related to a loss in the rigidity of actin filaments, rather than to a direct influence on the cross-linker. It should be noted that different actin preparations were found to exhibit a similar Ca^{2+}-dependent stimulation in apparent viscosity after gel filtration. This observation has also been reported by other investigators (Ohtaki et al., 1985).

Influence of Calcium on the Formation of α-Actinin–F-Actin Structures. Purified αA was tested for its ability to bundle actin filaments by negative staining and thin-section electron microscopy. When αA was incubated with F-actin at molar ratios lower than 1:35 in the absence of Ca^{2+}, the structural organization of actin filaments was not very different from that of negatively stained pure actin preparations. However, at molar ratios >1:30, small arrays of filaments were assembled in a loose and irregular network (not shown). As the amount of αA added to F-actin increased to a 1:5 molar ratio, large arrays of filaments became laterally aligned with one another (Figure 4A,B).

Incubation of αA with F-actin at a 1:10 molar ratio caused most of the filaments to become tightly combined in bundles. However, the bundles formed at a 1:5 αA to actin molar ratio were thicker than those obtained at a 1:10 ratio. This size difference could have been a consequence of the stabilizing effect exerted by unbound αA molecules (Meyer & Aebi, 1990).

The addition of Ca^{2+} to αA mixed with F-actin at a 1:5 molar ratio, at concentrations as high as 0.1 and 1 mM, only led to partial reduction in the maximal extent of bundle formation. Although large bundles predominated, smaller bundles of heterogeneous size were also detected. Moreover, the rare areas in which the size and number of bundles were reduced revealed the existence of an irregular and intricate network of filaments (Figure 4C,D).

The influence of Ca^{2+} on the ultrastructure of αA–F-actin bundles was examined in thin-sectioned samples. Transverse and longitudinal sections of bundles formed in the absence of Ca^{2+} showed that actin filaments were densely packed without any particular order of arrangement (Figure 5A,C). At a free concentration of 25 or 50 μM, Ca^{2+} did not apparently affect the morphology of the αA–F-actin bundles (panels D and E). Increasing the free Ca^{2+} concentration to 100 μM and higher resulted in the formation of disordered structures in which actin filaments were very intricate and loosely associated (compare panels B and G, and panels C and F, at two different magnifications).

Careful examination of bundles in Figure 5 (panels B and D) also revealed the existence of granular material dispersed along the actin filaments, namely, at points of proximity or contact between filaments. This material was not observed with actin filaments in the control sample (not shown). Likewise, this might represent the functional form of αA.

Studies on Binding of Calcium to α-Actinin. Since Ca^{2+} was found to affect αA–F-actin interactions only at relatively high concentrations, we decided to reexamine the Ca^{2+}-binding properties of macrophage αA. This protein was compared to calmodulin relative to its ability to bind Ca^{2+} on nitrocellulose filters using the dot blot procedure. This method has been successfully used for a number of Ca^{2+}-binding proteins including those of the annexin family which have a K_d in the 10 μM range (Klein et al., 1989). Graded amounts of native calmodulin and αA were bound to 0.12- and 0.45-μm nitrocellulose filters, respectively. The filters were then incubated with 2 μM $^{45}CaCl_2$ as described previously (Pacaud & Molla, 1987). This method allowed reproducible detection of ^{45}Ca binding at as low as 0.5 μg of calmodulin. However, no binding of ^{45}Ca to αA could be detected either in the presence or in the absence of Mg^{2+} when the filters were tested for their capacity to retain similar amounts of each protein (data not shown). Calmodulin has four Ca^{2+}-binding sites with a K_d of 3 and 50 μM in the presence of Mg^{2+} (Crouch & Klee, 1980). At the Ca^{2+} concentration used in this assay, the two high-Ca^{2+}-binding sites of calmodulin should have mainly contributed to the positive signal. The intensity of radioactive calmodulin on the autoradiograms, corrected for the difference in the molar mass of αA and calmodulin, led us to assume that binding of Ca^{2+} to αA in the assays could have been detected only if the affinity constant of this protein was 10-fold lower than that of calmodulin.

Other investigations on calcium binding were restricted to the effects of calcium ions on the αA conformation due to the limited amounts of purified αA. As nonmuscle αA does not have any chromophores in its presumptive Ca^{2+}-binding loops, energy transfer induced by metal binding cannot be observed by fluorescence. The last Trp residue present on the αA monomer is located at position 681, while the first amino acid residue of the nearest EF-hand-like motif is at position 714. There is, however, a Tyr residue at position 2 of the 12 amino acid long linking peptide between the 2 EF-hand-like domains (Baron et al., 1987; Arinura et al., 1988). The addition of increasing concentrations of Ca^{2+} to macrophage αA led to a decrease in the relative intensity of fluorescence emission of both Trp and Tyr residues without any shift in the wavelength. Under optimal conditions for calcium binding, i.e., without Mg^{2+} and K^+ or Na^+ ions, most of the spectral changes occurred between 10 and 100 μM free Ca^{2+}. When measured at the maximal emission wavelength, 334 nm for Tyr and 342 nm for Trp residues, the total extent of decrease was 6% for tryptophan and 9% for tyrosine. The data for both residues are illustrated in Figure 6. The addition of 1 mM Mg^{2+} to Ca^{2+}-free αA also led to a fluorescence

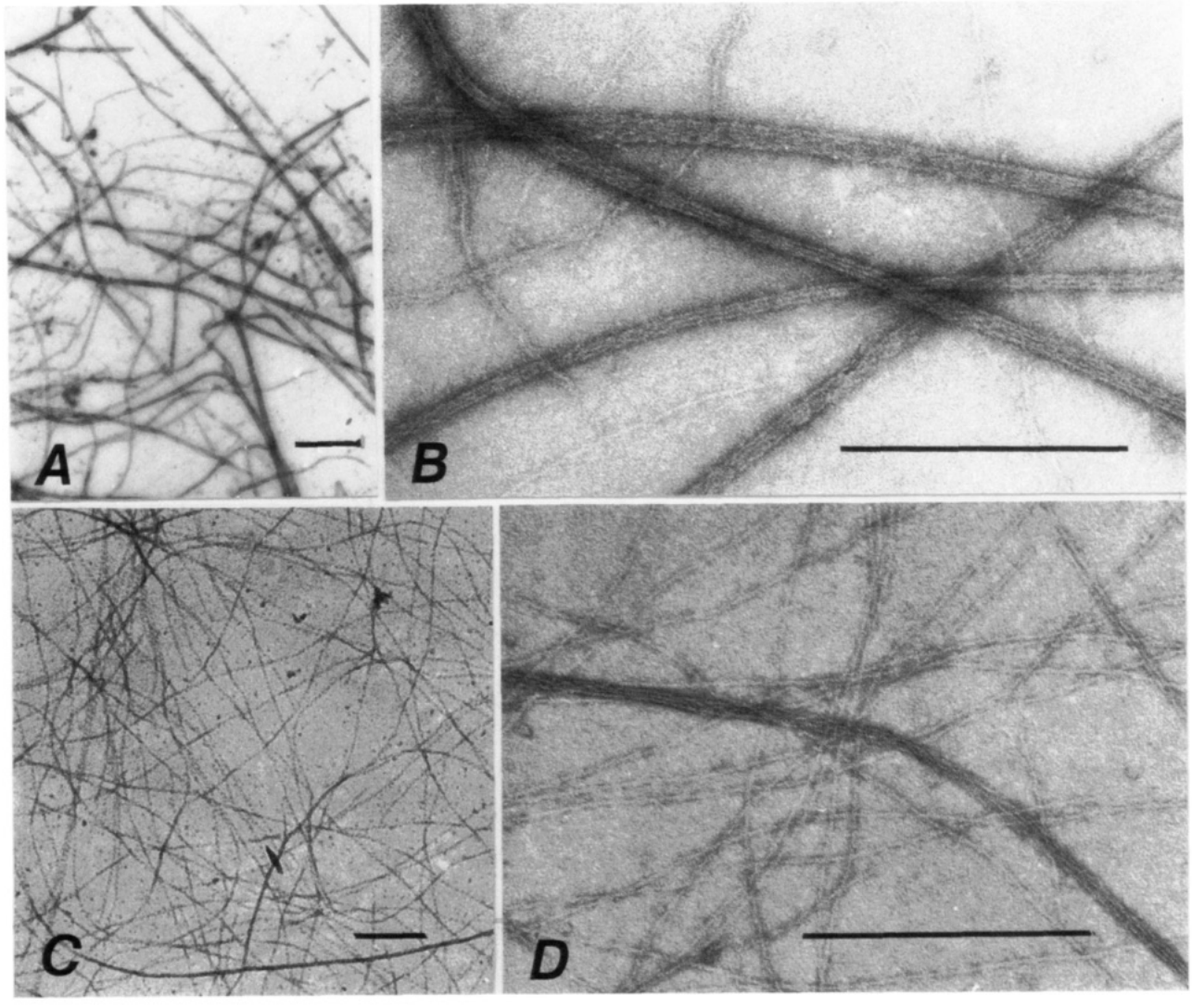

FIGURE 4: Electron micrographs of negatively stained preparations of F-actin and F-actin plus αA with and without Ca^{2+}. αA and F-actin were incubated for 3 h at 25 °C (at a molar ratio of about 1:5) under the conditions indicated in Table III. After dilution with 5 volumes of their respective incubation media, the samples were applied to grids and negatively stained with 1% aqueous uranyl acetate. Actin plus αA was incubated either without Ca^{2+} (A, B) or with 1 mM Ca^{2+} (C, D). The low magnifications in (C) illustrate the Ca^{2+}-induced arrangement of actin filaments in both networks and bundles (compare panels C and A). Magnifications are 20000 (A, C) and 82000 (B, D). Bars, 0.5 μM.

decrease, but the total decrease was not as great as that observed with Ca^{2+} (5% vs 9%) for Tyr residues. Subsequent addition of saturating amounts of calcium to the Mg–αA complex resulted in a small additional loss in the tryptophan and tyrosine fluorescence intensity, comparable to that maximally produced by calcium alone. The changes induced by Ca^{2+} and Mg^{2+} ions were no longer detectable in the presence of 140 mM KCl, i.e., at a physiological concentration of K^+ ions. These data together with Ca^{2+}-binding assays on nitrocellulose paper suggest that the Ca^{2+}-binding sites of αA might have an app K_d in the range of 10–100 μM, in the absence of Mg^{2+} and K^+. In the presence of these ions, binding of Ca^{2+} could have been detected by fluorescence only if this K_d range was increased 8–10-fold. Thus, under physiological ionic conditions, the app K_d of αA sites for Ca^{2+} is probably not higher than 80–100 μM.

DISCUSSION

The isolation and functional characterization of macrophage αA were part of our endeavor to understand the molecular mechanisms by which Ca^{2+} may regulate the structural organization of actin filaments. αA has been isolated from cytosolic protein by ammonium sulfate fractionation, DEAE-Trisacryl chromatography, and gel filtration. The purified protein migrated as a single major band during electrophoresis in SDS–polyacrylamide gels (Figure 1E). Other investigators (Bennet et al., 1984) reported the purification of macrophage αA from Triton-resistant cell structures. However, we did not follow their procedure since less than 30% of αA present in cell lysates was recovered in detergent-insoluble residues in our investigation. In addition, subsequent attempts at solubilization and purification from such cytoskeletal structures resulted in persistent contamination of αA with substantial amounts of actin (10–15%).

The protein isolated by the procedure described here exhibited the same molecular weight and isoelectric point as αA present in actin gel networks which had not undergone any chromatographic separation (Pacaud, 1986). Purifed αA assembled actin filaments in structures similar to those described for αA from chicken gizzard and *Acanthamoeba* (Jockush & Isenberg, 1981; Meyer & Aebi, 1990).

Binding of α-Actinin to F-Actin with and without Calcium. Under optimal conditions of interaction and in the absence of Ca^{2+}, 1 molecule of αA was able to bind maximally to

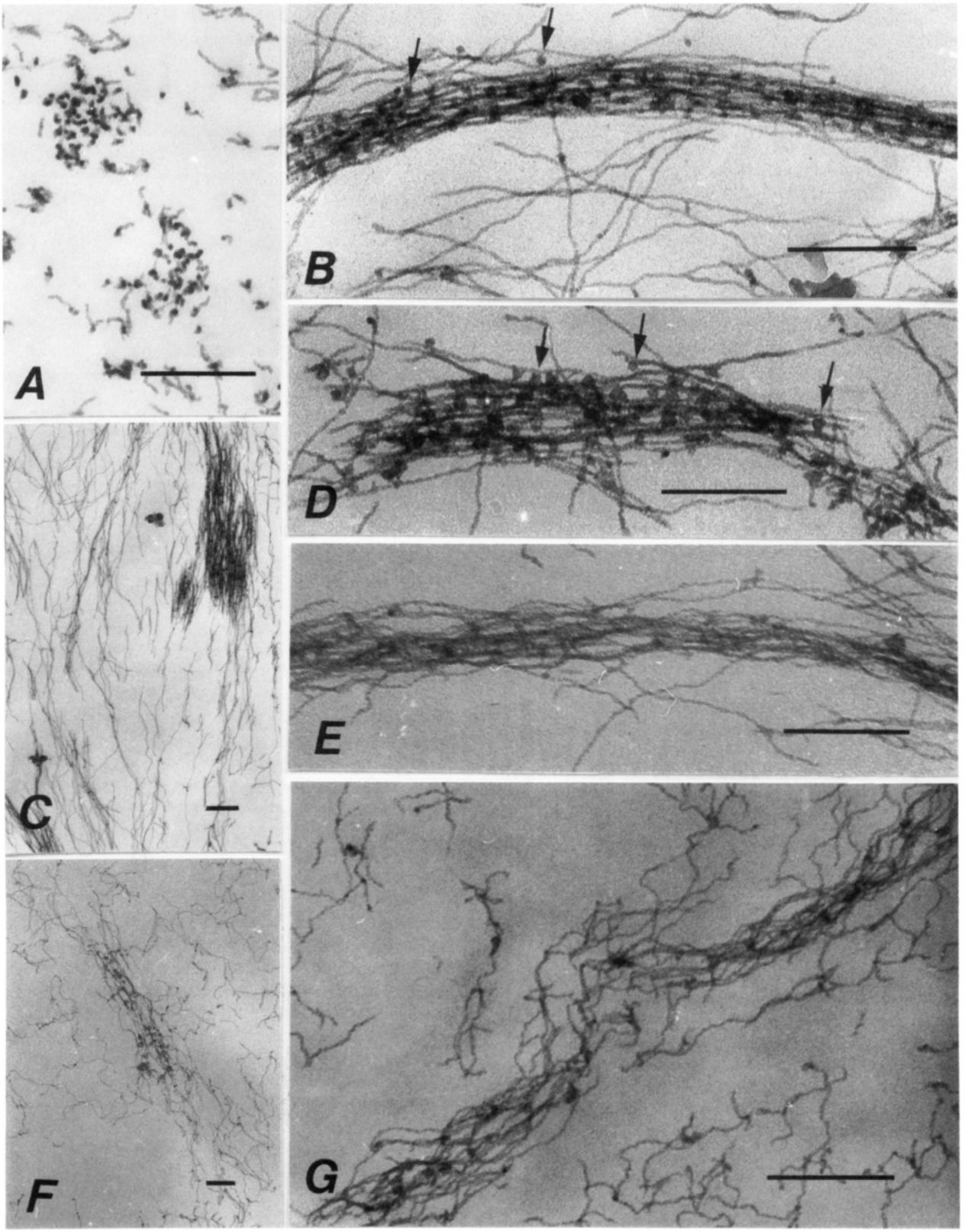

FIGURE 5: Electron micrographs of thin-sectioned actin bundles generated by αA in the absence and presence of Ca^{2+}. αA was mixed with F-actin at a molar ratio of about 1:5 either without Ca^{2+} (A, B, C) or with 25 (D), 50 (E) or 100 μM free Ca^{2+} (F, G) as indicated in Figure 5 (except that the incubation medium contained 4 mM $MgCl_2$ instead of 2 mM) and then fixed. Cross and longitudinal sections of the bundles formed in the absence of Ca^{2+} (A and C, respectively) revealed that most of the actin filaments lie in parallel with no regular order of arrangement. At $[Ca^{2+}] > 100$ μM, loose aggregations of actin filaments were observed (G) instead of compact bundles (B). The influence of Ca^{2+} on the general assembly of actin filaments by αA was also visualized at low magnifications (compare panels C and F). Longitudinal sections (at two different angles) in (B) and (D) showed the presence of granular particles between the filaments, possibly reflecting interfilament links. Magnifications are 20000 (C, F), 80000 (A), and 88000 (B, D, E. G). Bars, 0.25 μM.

about 12 molecules of actin monomers in the F-state, in agreement with that reported for αA from other nonmuscle cells (Meyer & Aebi, 1990). Two major classes of sites with app K_d values of 5.5 and 10 μM were involved in interactions between αA and F-actin at 25 °C (Figure 2). The Scatchard plots showed that the binding process, like the increase in

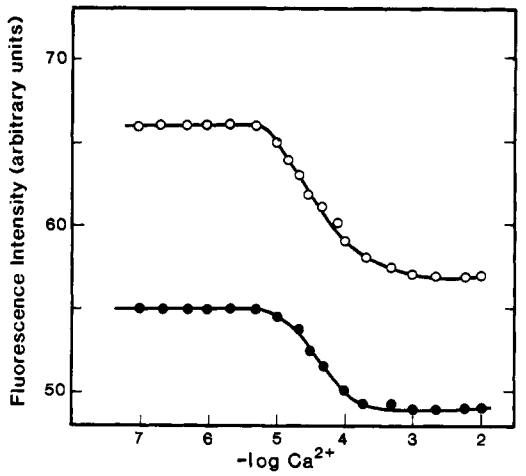

FIGURE 6: Decrease in the maximum intensity of fluorescence emission spectra of α-actinin on Ca^{2+} binding. Spectra were recorded with 0.25 μM α-actinin in 20 mM HEPES, 10%, glycerol and 1 mM dithiothreitol, pH 7.0 at 20 °C. Excitation was performed at 270 nm for tyrosine and at 290 nm for tryptophan residues. Fluorescence emission was measured at 334 nm for Tyr (○) and at 342 nm for Trp (●). In both cases, saturation was reached at about 0.1 mM free Ca^{2+}. The experimental points represent two different experiments. The presence of glycerol was required to keep the metal-free protein under native form even during fluorescence measurements. If not, reproducible results could not be obtained.

actin viscosity, occurred essentially in two steps. This suggests that in the absence of Ca^{2+} the binding of αA to the lowest affinity sites generally occurred when the highest affinity sites became saturated, i.e., when 1 molecule of αA was bound to 25–30 actin monomers. At a free concentration of 25 μM, Ca^{2+} did not alter the app K_d for the highest affinity sites. However, it slightly increased the number of cross-bridges since maximal binding was reached when 1 molecule of αA interacted with 8–9 actin monomers.

Since actin bundles were scarcely detected at αA to actin molar ratios lower than 1:30–1:35, binding of actin to high-affinity sites on αA was probably due to the initial cross-bridging of actin filaments, whereas binding to low-affinity sites could be essentially attributable to the bundling process. This interpretation is also supported by the observation that the viscosity of αA–F-actin mixtures, in the absence of Ca^{2+} ions, was found to increase linearly up to a critical αA:actin molar ratio of 1:30–1:35 (Figure 3). The results presented here contrast with those of Bennet et al. (1984). Starting with ^{125}I-labeled αA, they identified one class of actin-binding sites with an app K_d of 4 μM in the absence of Ca^{2+} and 77 μM in the presence of 0.1 mM Ca^{2+}. They also estimated a stoichiometry of 1 αA molecule per 2–3 actin monomers even though their binding experiments were performed at 37 °C, a temperature at which they could not detect any significant variations in the low-shear viscosity of αA–F-actin mixtures. Such discrepancies are difficult to explain in the absence of any information on the αA–F-actin structures which were formed in their experimental conditions. Iodination may alter the conformation of a portion of the αA molecule in such a way as to modify its interaction with F-actin. On the other hand, our αA preparations were not as potent as those of Bennet et al. (1984) with respect to their ability to affect the low-shear viscosity of F-actin. We found a 3.6-fold increase at αA:actin molar ratios varying between 0 and 1:35, and a 1.5-fold increase at molar ratios ranging between 1:35 and 1:12. These values can be compared with the >10-fold stimulation reported by these authors at molar ratios ranging from 1:115 to 1:80 at 21 °C. At first sight, these differences in effective concentrations might reflect differences in the affinity of the αA preparations for F-actin. However, such a high and sharp enhancement in actin viscosity appears to be more consistent with the formation of actin networks than actin bundles. Indeed, others have reported that the formation of actin bundles by villin (Matsudaira & Burgess, 1982) and muscle αA (Jockush & Isenberg, 1981) coincides with a decrease in the observed viscosity because a tangled actin network is more viscous than cross-bridged filaments in bundles.

Bennet et al. (1984) isolated macrophage αA by a procedure which included an enrichment step in cytoskeletal proteins and two chromatographic separations on hydroxylapatite and agarose. Starting with whole cell homogenates, they obtained αA with 380-fold purification. Starting from soluble cytosolic proteins, the procedure described here led to 550–600-fold purification. This represents a large difference in the degree of purity (about 3.5-fold) of αA prepared by the two methods. Accordingly, functional properties of αA might have been modified by the presence of an undetected protease and/or by other minor actin-binding proteins, such as filamin and gelsolin, which perhaps remained in their αA preparations. Filamin gives rise to the formation of actin networks, whereas gelsolin is a Ca^{2+}-binding protein which severs actin filaments in the presence of Ca^{2+} only (Yin & Stossel, 1980).

Influence of Ca^{2+} on the Ability of α-Actinin To Assemble Actin Filaments into Bundles. Bundling of actin filaments by α-actinin was demonstrated by low-speed sedimentation, low-shear viscosity, and most directly by electron microscopy. Low-speed sedimentation revealed that the maximal formation of bundles was inhibited slightly and gradually by increasing [Ca^{2+}] above a physiological range of 50–1000 μM (Table III). The amount of αA bound to F-actin remained relatively unchanged under these conditions. Negative-stain analysis of the αA–F-actin structures, generated at different Ca^{2+} concentrations, confirmed that bundle formation was only partially inhibited even in a millimolar range of Ca^{2+} (Figure 4). At a free concentration of 25 μM, Ca^{2+} had no effect on the ability of αA to increase the apparent viscosity of actin filaments in a concentration-dependent manner. However, at 100 μM and higher, Ca^{2+} caused a progressive decrease in actin viscosity when αA was added at bundling concentrations. Since this decrease was not associated with detectable changes in either filament length or number of free filaments, it might be due to a Ca^{2+}-induced loss in rigidity or organizational state of αA–actin structures. This interpretation is supported by electron microscopic examination of thin-sectioned samples. Disordered and loosely packed bundles were formed in the presence of 100 μM Ca^{2+}, in contrast to the ordered and compact bundles formed in the absence of Ca^{2+} (Figure 5). When evaluated at high centrifugal shear forces and in the presence of 25 μM Ca^{2+}, the apparent increase in the cross-bridging activity of αA (Figure 2) seems to indicate a loss in the stability of forming bundles, if disorganization of these weakly cross-linked structures is accompanied by a loss of αA binding. Evidence consistent with the release of bound αA being concomitant with the desintegration of αA–F-actin bundles comes from the studies of Meyer and Aebi (1990). They noted dissociation of αA–F-actin bundles by high shearing forces when free αA was removed or diluted out, as occurs during high-speed sedimentation.

The fact that Ca^{2+} gradually decreased both the sedimentability and viscosity of αA–F-actin structures up to the highest concentration tested deserves some comments. Studies on αA–F-actin interactions were all carried out in the presence

of K^+ and Mg^{2+} ions at concentrations that were found to reduce the binding to Ca^{2+} ions to αA molecules. Accordingly, the slow and progressive inhibition of actin bundling activity shown in Table III might have resulted from progressive saturation of low-affinity calcium-binding sites present on αA. However, αA molecules are not the only targets of Ca^{2+}, since the viscosity and low-speed sedimentability of actin filaments were already affected from 25 μM Ca^{2+}, and up to 1000 μM in the absence of αA. Other investigators have reported the binding of Ca^{2+} to actin filaments (Pope & Weeds, 1986) and found that it decreases their structural stability (Uyemura et al., 1978). The binding of cations to oligomeric actin has not yet been determined, but monomeric actin binds Ca^{2+} with a K_d of about 10 μM, and Mg^{2+} in the range of 10–50 μM (Frieden et al., 1982; Zimmerle et al., 1987). A loss of rigidity of actin filaments could alter the position of cross-bridging points between adjacent filaments and hence give rise to the formation of loose and disordered αA–F-actin bundles as detected in the presence of Ca^{2+}. On the other hand, the fact that Ca^{2+} inhibited neither the binding of αA to actin nor the formation of initial cross-bridges raises the possibility that, under Ca^{2+}-bound and highly cross-linked form, actin filaments might reduce the affinity of αA molecules for Ca^{2+}.

Binding of Calcium Ions to α-Actinin. In the absence of Mg^{2+} and K^+ ions, the binding of calcium to αA, at concentrations ranging from 10 to 100 μM free Ca^{2+}, induced significant perturbations in the environment of Tyr and Trp residues. The extent of these perturbations could not be evaluated since the αA monomer contained 14 Trp and 19 Tyr residues, with only 1 Tyr residue located in the vicinity of the 2 EF-hand-like regions. It is known that the indole group of tryptophan is a more sensitive chromophore than the phenol ring of tyrosine. Likewise, the observed greater decrease in fluorescence intensity of Tyr residues than that of Trp residues suggests that these spectral perturbations arise from specific interactions of Ca^{2+} ions with Ca^{2+}-binding sites. The position and distance of the last Trp residue on the αA monomer indicate that the Ca^{2+}-induced conformational changes were not limited to the EF-hand-like domains. Since binding of Mg^{2+} to αA gave rise to the same type of spectral perturbations in the environment of Tyr and Trp residues as Ca^{2+}, these two bivalent cations might act by a similar mechanism. Mg^{2+} and Ca^{2+} compete for binding to identical sites on calmodulin (Crouch & Klee, 1980; Haeich et al., 1981). The identical effect of KCl on the fluorescence emission spectrum of Tyr and Trp residues is also indicative of monovalent cations binding to αA. It is possible that K^+ ions interact nonspecifically with negative charges of the protein and thus decrease its Ca^{2+} or Mg^{2+} affinity without interacting with the Ca^{2+}-binding sites. The presence of low-affinity sites for Ca^{2+} ions detected in these studies is in agreement with the weak inhibitory influence of Ca^{2+} on αA–F-actin interactions.

The EF-hand Ca^{2+}-binding sites of proteins in the calmodulin superfamily come in pairs (Persechini et al., 1989). Single EF-hand Ca^{2+}-binding sites have a very low affinity for Ca^{2+} unless they are able to dimerize in the presence of Ca^{2+} (Reid, 1987; Shaw et al., 1990). On the basis of these findings together with a recent discovery on the critical role of the Glu Ca^{2+}-ligation residue at position 12 of calmodulin loops, it could be speculated that the loop in the second EF-hand like motif of αA (see the introduction) accounts for both the weak Ca^{2+}-binding properties of this protein and the loss in Ca^{2+}-selective binding. Indeed, studies on point mutations in calmodulin have demonstrated that the Glu → Ala substitution at position 12 in one of each pair of Ca^{2+}-binding loops greatly reduces Ca^{2+} binding at interacting sites but does not alter Mg^{2+} binding (Haiech et al., 1991). Similar findings with two other related Ca^{2+}-binding site mutants of calmodulin have also been reported more recently (Maune et al., 1992).

Using equilibrium dialysis, Bennet et al. (1984) found that macrophage αA binds 4 mol of Ca^{2+}/mol of protein, with an app K_d of 4 μM in the presence of 2 mM $MgCl_2$ and 100 mM KCl. Their protein preparations and evaluations were based on different protocols; thus, no rigorous comparisons can be made. In their case, cell lysis with Triton X-100 might have led to incomplete removal of membrane phospholipids from the partially purified protein. They also used αA solutions that were extensively dialyzed against 50 μM EGTA. Metal-binding proteins like parvalbumin and calmodulin are known to bind EGTA with a relatively high affinity (Haiech et al., 1979, 1980). If αA has such a capacity, this might have shifted its Ca^{2+}-binding properties, leading to an apparent increase in the affinity constant for Ca^{2+}. Equilibrium dialysis is not a suitable method for direct ligand-binding measurements with low-affinity proteins, and this is particularly true for those which have a high molecular weight (Ridlington & Butler, 1969).

Is α-Actinin a Ca^{2+}-Regulated Actin-Binding Protein? In previous studies, we demonstrated that Ca^{2+}, at concentrations of 0.3–3 μM, controls the association of three cytoskeletal proteins (a 70-kDa protein, fodrin, and gelsolin) with actin gel networks formed in macrophage cell extracts whereas it does not affect the behavior of αA (Pacaud & Molla, 1987; Pacaud & Harricane, 1987). We confirmed here that Ca^{2+} did not have any significant effect on the interactions of purified αA with F-actin and presented evidence suggesting that αA binds Ca^{2+} with low affinity. This conclusion contrasts with the generally accepted idea that vertebrate nonmuscle αA is a Ca^{2+}-regulated actin-binding protein. However, the effect of Ca^{2+} on the functional properties of this protein was not investigated in detail. The differences in Ca^{2+} sensitivity exhibited by muscle αA and platelet or brain αA have essentially been based on differences in high-speed sedimentability of αA–F-actin structures formed in the absence or presence of 2 or 2.5 mM Ca^{2+} (Rosenberg et al., 1981; Duhaiman & Bamburg, 1984). Moreover, except for a study on αA from rat liver (Ohtaki et al., 1985), investigations on Ca^{2+} sensitivity of αA from various vertebrate cells have all been performed with actin preparations not previously cleared of protein contaminants by gel filtration, and there have been no reports on the morphology of αA–F-actin structures. Thus, no clear conclusions can be drawn on αA–F-actin interactions in the absence of electron microscopy studies. Such analyses were of great help to us not only for understanding biochemical data but also for checking the purity and activity of protein preparations. On the other hand, it is important to point out that vertebrate αA isolated from various nonmuscle cells exhibited large differences in their ability to assemble actin filaments. αA from HeLa cells (Burridge & Feramisco, 1981b), rat liver (Kuo et al., 1982; Ohtaki et al., 1985), and macrophages (Bennet et al., 1984) was found to have a gelation activity, or capacity to form actin networks instead of bundles, approximately 10-fold higher than αA from brain (Duhaiman & Bamburg, 1984) and platelets (Landon et al., 1985). Comparing the properties of αA from chicken gizzard, *Acanthamoeba*, and *Dictyostelium*, Meyer and Aebi (1990) have demonstrated that the bundling of actin filaments by αA

is dependent on its molecular length. Likewise, a large increase in the gelation capacity of αA may be the consequence of proteolytic degradation which might occur either during protein purification or during incubation with F-actin. This may also explained why most αA isforms were found to be more active at 0 °C than at higher temperatures. It is worth noting that Gache et al. (1984) reported that, in contrast to muscle αA, platelet αA can be partially degraded by an endogenous Ca^{2+}-activated neutral protease. This could explain the reported differences in Ca^{2+} sensitivity of muscle and vertebrate nonmuscle αA. Indeed, we were faced with the difficulties of completely separating αA from other actin-binding proteins, and of avoiding its proteolytic degradation during purification. In addition to artifacts due to incomplete purification of αA and/or actin, problems related to the Ca^{2+}-binding properties of F-actin may have led to the erroneous concept that interactions of αA with F-actin are regulated by Ca^{2+} binding to αA within cells. However, the data presented here do not rule out the possibility that the affinity of αA for F-actin could be indirectly regulated through its interactions with other proteins. The observation that Ca^{2+} affects neither the association of αA with F-actin in cytosolic extracts (Pacaud & Molla, 1987) nor its partition between cytosolic and membrane proteins (unpublished data) does not favor the hypothesis of direct interactions with other Ca^{2+}-binding proteins. The intracellular distribution of αA molecules might well be controlled by a complex regulation. Indeed, Burn et al. (1985) reported that stimulation of platelets by thrombin led to the formation of a stoichiometric complex of αA with both diacylglycerol and palmitic acid, with a parallel increase in actin bundle formation. Since thrombin also induces a rise in free Ca^{2+} concentrations, this raises the interesting possibility that the hydrophobicity and lipid-binding affinity of αA might change upon Ca^{2+} binding. Reciprocally, in a lipid-bound form, αA might have a different affinity for both Ca^{2+} and Mg^{2+}.

Dictyostelium αA was found to be inhibited from interacting with F-actin by micromolar concentrations of free Ca^{2+} (Condeelis & Vahey, 1982), but direct Ca^{2+}-binding data have not yet been reported. However, its predicted amino acid sequence revealed two EF-hand motifs which appear to have the ligation residues expected for Ca^{2+}-binding sites of high affinity (Noegel et al., 1987). This raises the possibility that αA's of various origins are derived from a common ancestral Ca^{2+}-binding protein whose Ca^{2+}-binding properties have been lost during evolution.

ACKNOWLEDGMENT

We thank Dr. Claude Roustan for stimulating discussions and help with fluorescence measurements and Martine Peytavin and Patricia Eustaquio for their expert editorial assistance. We are particularly grateful to Professor Jacques Haeich for helpful advice on Ca^{2+}-binding experiments and critical reading of the manuscript.

REFERENCES

Arimura, T., Suzuki, T., Yanagisawa, M., Imamura, M., Hamada, Y., & Masaki, T. (1988) *Eur. J. Biochem. 177*, 649–655.

Autric, A., Ferraz, C., Kilhoffer, M. C., Cavadore, J. C., & Demaille, J. G. (1980) *Biochim. Biophys. Acta 631*, 139–147.

Baron, M. D., Davison, M. D., Jones, P., & Critchley, D. R. (1987) *J. Biol. Chem. 262*, 17623–17629.

Bennett, J. P., Zaner, K. S., & Stossel, T. P. (1984) *Biochemistry 23*, 5081–5086.

Blanchard, A., Ohanian, V., & Critchley, D. (1989) *J. Muscle Res. Cell Motil. 10*, 280–289.

Bradford, M. M. (1976) *Anal. Biochem. 72*, 248–254.

Burn, P., Rotman, A., Meyer, R. K., & Burger, M. M. (1985) *Nature 314*, 469–472.

Burridge, K., & Feramisco, J. R. (1981a) *Cold Spring Harbor Symp. Quant. Biol. 46*, 613–623.

Burridge, K., & Feramisco, J. R. (1981b) *Nature 294*, 565–567.

Condeelis, J., & Vahey, M. (1982) *J. Cell Biol. 94*, 466–471.

Craig, S. W., & Pollard, T. D. (1982) *Trends Biochem. Sci. 7*, 88–92.

Crouch, T. H., & Klee, C. B. (1980) *Biochemistry 19*, 3962–3968.

Duhaiman, A. S., & Bamburg, J. R. (1984) *Biochemistry 23*, 1600–1608.

Ebashi, S., Ebashi, F., & Maruyama, K. (1964) *Nature (London) 203*, 645–646.

Endo, T., & Masaki, T. (1982) *J. Biochem. 92*, 1457–1468.

Frieden, C. (1982) *J. Biol. Chem. 257*, 2882–2886.

Gache, Y., Landon, F., Touitou, H., & Olomucki, A. (1984) *Biochem. Biophys. Res. Commun. 124*, 877–881.

Haiech, J., Derancourt, J., Pechere, J. F., & Demaille, J. G. (1979) *Biochemistry 18*, 2752–2758.

Haiech, J., Vallet, B., Aquaron, R., & Demaille, J. (1980) *Anal. Biochem. 105*, 18–23.

Haiech, J., Klee, C. B., & Demaille, J. G. (1981) *Biochemistry 20*, 3890–3897.

Haiech, J., Kilhoffer, M. C., Lukas, T. J., Craig, T. A., Roberts, D. M., & Watterson, D. M. (1991) *J. Biol. Chem. 266*, 3427–3431.

Hartwig, J. H., & Stossel, T. P. (1981) *J. Mol. Biol. 145*, 563–581.

Howard, T. H., & Oresajo, C. O. (1985) *J. Cell Biol. 101*, 1078–1085.

Jockusch, B. M., & Isenburg, G. (1981) *Proc. Natl. Acad. Sci. U.S.A. 78*, 3005–3009.

Klein, D. P., Jongstra-Bilen, J., Ogryzlo, K., Chong, R., & Jongstra, J. (1989) *Mol. Cell. Biol. 9*, 3043–3048.

Kuo, P. F., Mimura, N., & Asano, A. (1982) *Eur. J. Biochem. 125*, 277–282.

Laemmli, U. K. (1970) *Nature (London) 227*, 680–685.

Landon, F., Gache, Y., Touitou, H., & Olomucki, A. (1985) *Eur. J. Biochem. 153*, 231–237.

Lazarides, E., & Burridge, K. (1975) *Cell 6*, 289–298.

Lowry, O. H., Rosebrough, N. J., Farr, A. L., & Randall, R. J. (1951) *J. Biol. Chem. 193*, 265–275.

MacLean-Fletcher, S. D., & Pollard, D. (1980) *J. Cell Biol. 85*, 414–428.

Matsudaira, P. T., & Burgess, D. R. (1982) *J. Cell Biol. 92*, 648–656.

Maune, J. F., Klee, C. B., & Beckingham, K. (1992) *J. Biol. Chem. 267*, 5286–5295.

Meyer, R. K., & Aebi, U. (1990) *J. Cell Biol. 110*, 2103–2024.

Noegel, A., Witke, W., & Schleicher (1987) *FEBS Lett. 221*, 391–396.

Ohtaki, T., Tsukita, S., Mimura, N., Tsukita, S., & Asano, A. (1985) *Eur. J. Biochem. 153*, 609–620.

Omann, G. M., Allen, R. A., Bokoch, G. M., Painter, R. G., Traynor, A. E., & Sklar, L. A. (1987) *Physiol. Res. 67*, 285–322.

Pacaud, M. (1986) *Eur. J. Biochem. 156*, 521–530.

Pacaud, M., & Harricane, H. (1987) *J. Cell Sci. 88*, 81–94.

Pacaud, M., & Molla, A. (1987) *Eur. J. Biochem. 165*, 139–145.

Pavalko, F. M., & Burridge, K. (1991) *J. Cell Biol. 114*, 481–491.

Persechini, A., Moncrief, N. C., & Kretsinger, R. H. (1989) *Trends Neurol. Sci. 12*, 462–467.

Pollard, T. D., & Cooper, J. A. (1986) *Annu. Rev. Biochem. 55*, 987–1035.

Pope, B., & Weeds, A. (1986) *Eur. J. Biochem. 161*, 85–93.

Reid, R. E. (1987) *Biochemistry 26*, 6070–6073.

Ridlington, J., & Butler, L. G. (1969) *J. Biol. Chem. 244*, 777–779.

Rosenberg, S., Stracher, A., & Burridge, K. (1981) *J. Biol. Chem. 256*, 12986–12991.

Shaw, G. C., Hodges, R. S., & Sykes, B. D. (1990) *Science 249*, 280–283.

Sklar, A. L., Omann, G. M., & Painter, R. G. (1985) *J. Cell Biol. 101*, 1161–1166.

Spudich, J. A., & Watt, S. (1971) *J. Biol. Chem. 246*, 4866–4871.

Stossel, T. P., Chaponnier, C., Ezzel, R. M., Hartwig, J. H., Janmey, P. A., Kwiatkowski, D. J., Lind, S. E., Smith, D. B., Southwick, F. S., Yin, H. L., & Zaner, K. S. (1985) *Annu. Rev. Cell Biol. 1*, 353–402.

Strynadka, N. C. J., & James, M. N. G. (1989) *Annu. Rev. Biochem. 58*, 951–980.

Uyemura, D. G., Brown, S. S., & Spudich, J. A. (1978) *J. Biol. Chem. 253*, 9088–9096.

Wallraff, E., Schleicher, M., Modersitzki, M., Rieger, D., Isenberg, G., & Gerich, G. (1986) *EMBO J. 5*, 61–67.

Weeds, A. (1982) *Nature (London) 296*, 811–816.

Witke, W., Schleicher, M., Lottspeich, F., & Noegel, A. (1986) *J. Cell Biol. 103*, 969–975.

Yin, H. L., & Stossel, T. P. (1980) *J. Biol. Chem. 255*, 9490–9493.

Zimmerle, C. T., Patane, K., & Frieden, C. (1987) *Biochemistry 26*, 6545–6552.